Journal of Neonatal Surgery
ISSN(Online): 2226-0439
Vol. 14, Issue 32s (2025)
https://www.jneonatalsurg.com

OPEN ACCESS

Hybrid NiO–Bi(III) Schiff Base Complexes: Spectroscopic Insight into Protein Binding and Enhanced Antibacterial Activity

S. Rama pandian[a,b], A. Mathavan*[a], C. Vedhi*[a]

[a]Department of Chemistry, V. O. Chidambaram College, Tuticorin 628 008, Tamil Nadu, India

[b]Research Scholar (Registration Number: 17232232031011), V. O. Chidambaram College, Tuticorin - 628 008 (affiliated) Manonmaniam Sundaranar University, Abishekapatti, Tirunelveli, Tamil Nadu 627 012, India

***Corresponding Author**

Email.ID: abhimathavan@gmail.com

Email.ID: cvedhi23@gmail.com

Cite this paper as: S. Rama pandian, A. Mathavan, C. Vedhi, (2025) Hybrid NiO–Bi(III) Schiff Base Complexes: Spectroscopic Insight into Protein Binding and Enhanced Antibacterial Activity. *Journal of Neonatal Surgery*, 14 (32s), 5346-5355.

ABSTRACT

This study shows the successful creation of new hybrid nanomaterials by combining Bi(III) Schiff base complexes from nitro-Salen ligands with NiO nanoparticles. Spectroscopic techniques like FT-IR and UV-Vis confirmed strong coordination and improved optical properties, including a reduced band gap of 2.12 eV. XRD and FE-SEM analyses displayed porous, nanoscale structures with clear shapes. These hybrids showed strong interactions with serum proteins BSA, which was evident through fluorescence quenching and molecular docking, with a binding energy of –8.1 kcal/mol. Notably, the antibacterial activity of the hybrids increased significantly, especially when combined with Ampicillin. Overall, these results emphasize the potential of these multifunctional materials in biomedical uses like biosensing, targeted drug delivery, and antimicrobial treatments.

Keywords: *Schiff base complexes, Bismuth (III), NiO hybrids, Optical properties, Protein binding, Antibacterial activity.*

1. INTRODUCTION

Metal-organic hybrids made from Schiff base ligands have gained more attention for their versatility in catalysis, sensing, biomedical uses, and drug delivery [1]. Bismuth (Bi^{3+})-based complexes stand out as promising options due to their low toxicity, good coordination behavior, and biological compatibility [3, 4]. When combined with nickel oxide (NiO), which is a p-type semiconductor known for its high stability and surface conductivity [5], these hybrids can show improved properties. Adding nitro groups to the Schiff base ligand framework can also help fine-tune electron transport and target-specific interactions [7]. The synergy between these components supports superior optical and electrochemical performance, particularly through metal-to-ligand charge transfer and π–π* transitions [8, 9]. Beyond their physicochemical properties, Bi-based complexes have also demonstrated effective antibacterial activity and strong interactions with biomolecules, which are largely attributed to their polarizability and structural adaptability [10]. Considering the critical role of protein binding especially with serum proteins like BSA and HAS in determining the pharmacokinetics of therapeutic agents [11], this work aims to synthesize and characterize a Nitro Salen–Bi(III) complex and its NiO-integrated hybrid. We explore their structural features, binding behavior, and antibacterial properties, with particular focus on their synergistic action when combined with Ampicillin.

2. MATERIAL AND METHODOLOGY

Materials

$Bi(NO_3)_3$, $NiCl_2$.$6H_2O$, NaOH, methanol, ethanol, salicylal aldehyde, nitro salicylaldehyde, ethylene diamine are purchased from e-merk and used as such.

Preparation of NiO

5.94 g (0.1M) of $NiCl_2$.$6H_2O$ along with 1 g of NaOH pellet added and makeup in 250 ml of volume then stirring continuously for two hours, Then green gel was formed and washed with water along with ethanol and dried. Then

Calcination process was carried out at 450 c in oven, Finally, the green coloured sample changed into black powder and grained with morter which was in nano sized.

Preparation of salen;

The salen ligand was prepared by refluxing of a mixture of 3.66 g (3.1ml) of salicylal aldehyde and 0.9g(1.0ml) of ethylene diamine(1:2 ratio) in 150 ml of methanol for one hour.

After completion of reaction the yellow crystalline solid (Salen) was collected and washed with cold methanol and dried in air.

Preparation of 5,5' Dinitro salen:

3.04 gm of 5 nitro salicylaldehyde refluxing with 0.9g (1.0ml)of ethylene diamine (1:2 ratio) in 150 ml of methanol for one hour. The pale yellow crystalline solid (Nitro salen) was collected and washed with cold methanol and dried in air.

Preparation of Bismuth salen complex (SBC):

0.9693g of $Bi(NO_3)_3$ in ethanol refluxed with 0.5366g of salen for 2 hours with constant stirring in oil bath and the product was collected by filtration and washed with cold ethanol for 10 minutes and dried in air, then white coloured complex was obtained

Preparation of 5,5' Nitro salen Bismuth complex (Nitro SBC):

0.9693g of $Bi(NO_3)_3$ in ethanol refluxed with 0.4852g of Nitro salen for 2 hours with constant stirring in oil bath and the product was collected by filtration and washed with cold ethanol for 10 minutes and dried in air, then pale yellow coloured complex (Nitro SBC)was obtained.

Preparation of NiO -Nitro SBC nano composite:

By using Co-precipitation method, nano sized metal oxide (NiO) dissolved in base medium like NaOH (precipitating medium) was mixed with prepared 5,5'Nitro salen Bismuth Complex(Nitro SBC)in fixed proportion of 1:1 which results black coloured gelly nano composites through Calcination at 120 C along with Centrifugation of 100 rpm, The dried NiO-Nitro SBC was obtained.

Characterization

The FT-IR spectra were recorded using computer controlled Thromofisher scientific instrument. Computer controlled JASCO V-530 and FP-8300 was used to study UV-VIS spectral and fluorescence behavior. XRD measurements were made by Panalytical X'Pert Powder X' Celerator Diffractometer, measurement range: 10 to 80 degree in 2θ and particle size was calculated using Scherrer's equation. The FESEM measurements were carried by JEOL JSM-6700F field emission scanning electron microscope.

3. RESULTS AND DISCUSSION

FT-IR Studies

Figure 1 shows the FT-IR spectra of NiO, the Nitro Salen Bi complex, and their hybrid material. The spectrum of pure NiO displays distinct absorption bands that correspond to O–H stretching, H–O–H bending, and the Ni–O lattice vibration, confirming successful nanoparticle synthesis [12, 13]. In contrast, the Bi complex reveals prominent peaks related to the C=N and NO_2 functional groups [14, 15]. When hybridization occurs, we observe noticeable spectral shifts. Specifically, the O–H band moves from 3435 to 3423 cm^{-1}, the C=N stretch shifts from 1627 to 1614 cm^{-1}, and NO_2 vibrations also change. These shifts indicate strong coordination between the ligand and the NiO surface [16]. The retention of the Ni–O peak suggests that the main NiO structure remains intact. Overall, these changes confirm the formation of the hybrid through metal–ligand bonding and electrostatic interactions.

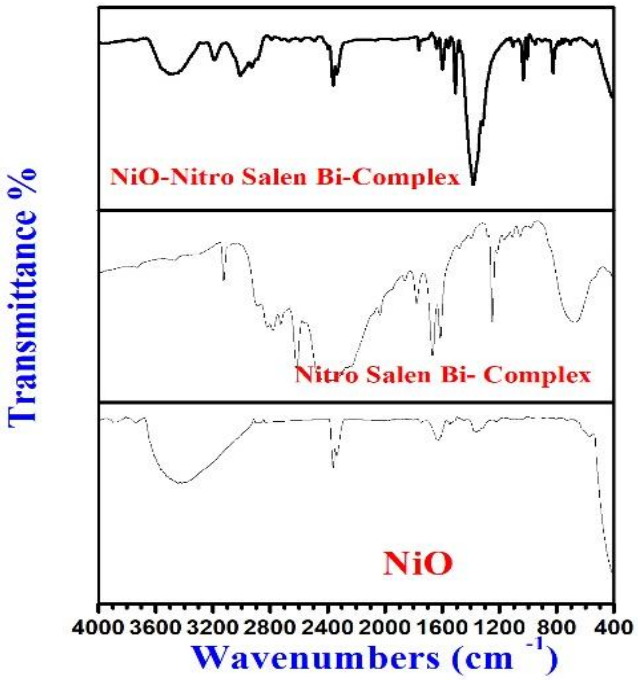

Fig.1. FT-IR Spectrum of NiO, Nitro salen Bi complex and NiO-Nitro salen Bi complex

UV-Vis Studies

Figure 2 shows the UV-Vis absorption spectra of NiO, the Nitro Salen Bi complex, and their hybrid. NiO has strong absorption in the 200-400 nm range. This is mainly due to charge transfer from O^{2-} to Ni^{2+} ions [17, 18]. In contrast, the Bi complex shows characteristic π-π* and n-π* electronic transitions that extend up to 450 nm [19]. The hybrid material combines these features and improves them, with broadened absorption reaching 500 nm and a distinct shoulder around 310 nm. This suggests a strong interaction between NiO and the ligand, as well as better optical activity [20]. Band gap analysis using Tauc plots (Figures 3) further supports these findings. The hybrid has a band gap of 2.12 eV, which is lower than NiO 2.42 eV and the Bi complex's 2.23 eV, but higher than pure Nitro Salen's 1.93 eV [21-25]. This decrease in band gap shows improved charge transfer ability, making the hybrid a good candidate for photocatalysis and optical sensing applications.

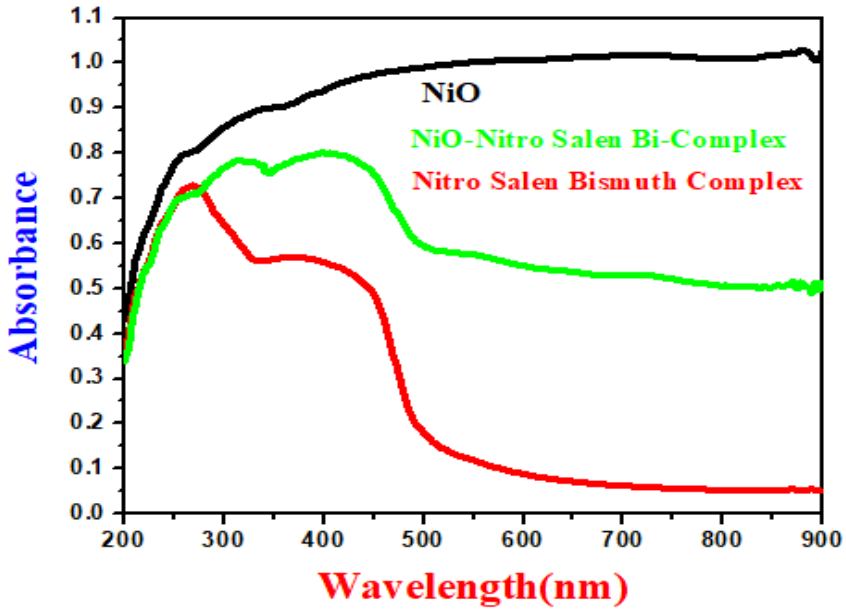

Fig.2. UV-Vis Spectrum of NiO, NiO-Nitro Salen Bi complex and Nitro Salen Bi complex

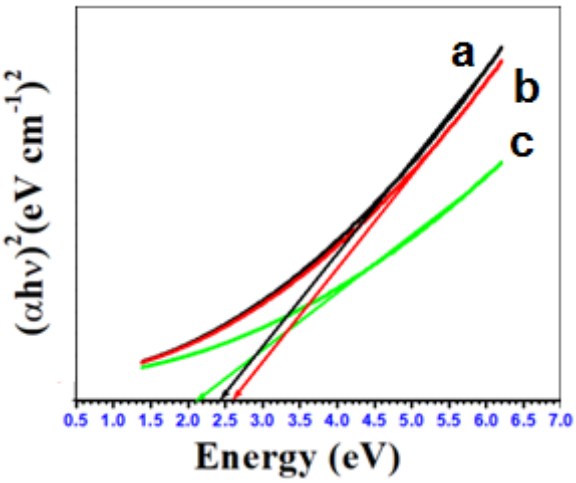

Fig 3. Band gap curve of a) NiO, b) Nitro-salen complex and c) NiO Nitro-Bi-Salen complex

FE-SEM Studies

Figure 4 shows quasi-cubic NiO particles ranging from 200 to 500 nm. They have smooth surfaces and high crystallinity. Their uniformity and low agglomeration indicate controlled synthesis, which improves surface area and electrochemical activity [26]. Figure 6 displays porous, aggregated Nitro Salen Bi nanoparticles smaller than 100 nm. They are ideal for electrochemical applications due to their high surface area and active site exposure. Agglomeration likely comes from surface energy, which aligns with earlier reports [27–29]. Figure 7 shows NiO–Nitro Salen Bi with porous, cauliflower-like particles between 50 and 100 nm that form a 3D network. Bismuth and Nitro Salen likely guided NiO growth, leading to better electrocatalytic properties [30, 31].

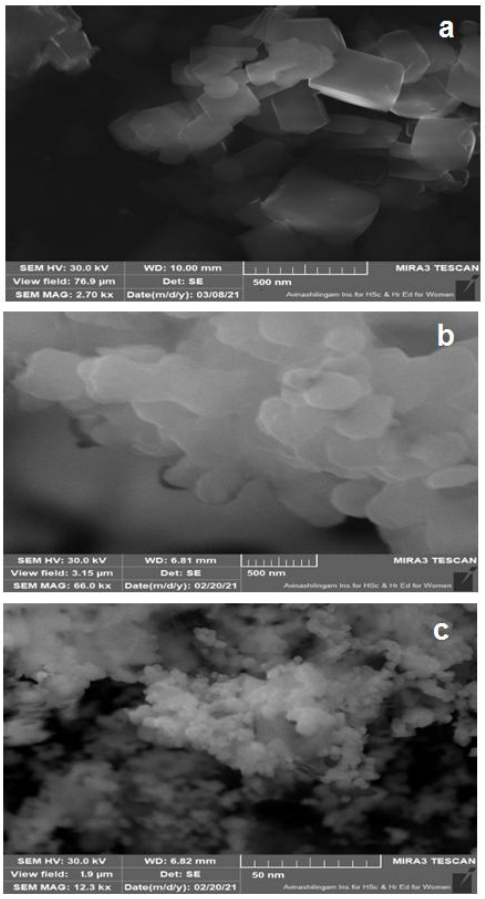

Fig.4. FE-SEM image of a) NiO b) Nitro Salen Bi complex c) NiO- Nitro Salen Bi complex

XRD Studies

XRD analysis (Figure 5) was used to assess the crystallinity and structural changes in the synthesized materials. NiO (Figure 8) shows sharp peaks at 2θ = 37.3°, 43.3°, 62.9°, 75.4°, and 79.4°. These peaks correspond to the (111), (200), (220), (311), and (222) planes of face-centered cubic NiO (JCPDS 47-1049) [32]. This indicates high crystallinity and a preferred (200) orientation. The Nitro Salen–Bi complex (Figure 9) displays new peaks at 13.2°, 18.9°, 26.4°, 30.1°, 38.4°, and 47.6°. The intensity of the original ligand peaks is reduced, confirming Bi(III) coordination and the formation of new crystalline areas [33]. The NiO–Nitro Salen–Bi complex (Figure 10) shows broad, low-intensity peaks, which suggest a semi-crystalline or amorphous hybrid structure. Weak reflections at approximately 37.1° and 43.1° from NiO remain, but broader peaks at 18.3°, 27.5°, 31.0°, and 47.8° reflect disorder in the organic–inorganic matrix caused by Bi inclusion [34]. Crystallite sizes, calculated using the Debye–Scherrer equation, decrease throughout the series: NiO (37 nm at 43.3°) [35], Nitro Salen–Bi (19 nm at 30.1°) [36], and NiO–Nitro Salen–Bi (18 nm at 43.1°) [37]. This decrease suggests lattice strain, increased disorder, and factors related to hybrid formation. These changes may improve surface activity and electron transport for uses in catalysis or sensing.

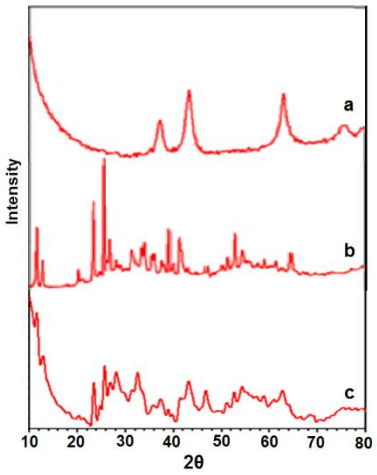

Fig.5. XRD behaviour of NiO, Nitro Salen Bi complex and NiO-Nitro Salen Bi complex

Binding Studies of Bovine Serum Albumin (BSA) with Different Complexes

BSA binding with NiO, Nitro Salen-Bi, and NiO-Nitro Salen-Bi complexes was studied using UV-Vis and fluorescence spectroscopy. NiO displayed a mild red shift at 277 nm and fluorescence quenching at 302 nm (Figure 7-8). This indicates moderate interaction with a binding constant of Kb = 1.24×10^4 M^{-1} via a static mechanism [38]. The Nitro Salen-Bi complex caused a shift from 220 to 214 nm and showed dual emissions at 324 and 448 nm. This suggests stronger binding and multi-site interaction, with a binding constant of Kb = 2.37×10^4 M^{-1}, aided by Bi^{3+} coordination [39]. NiO-Nitro Salen-Bi exhibited the most significant spectral changes, including new peaks at 250 and 258 nm, broadened emissions at 360 and 386 nm, and the highest binding constant of Kb = 3.12×10^4 M^{-1}. These results reflect improved interaction through the combined effects of NiO and Bi^{3+} [40]. As shown in Table 1, binding strength increased with the incorporation of metals, driven by electrostatic forces, polar interactions, and structural rearrangement near tryptophan residues.

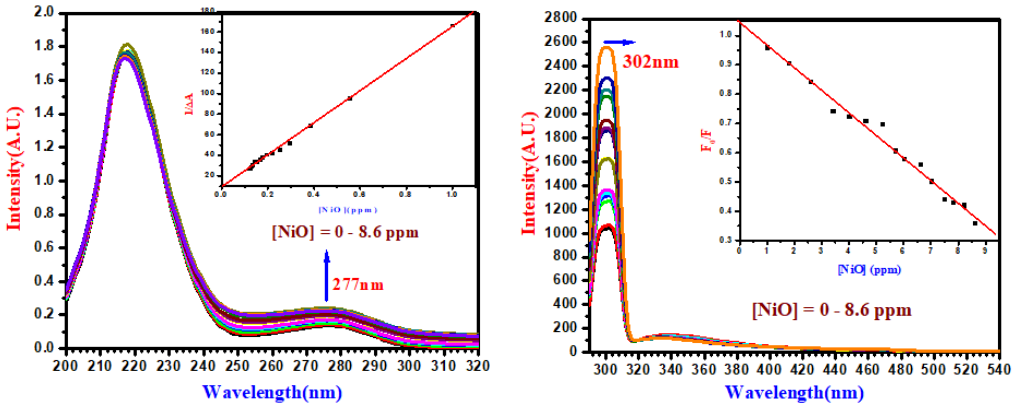

Fig.6 a) absorption and b) emission spectra of NiO-BSA

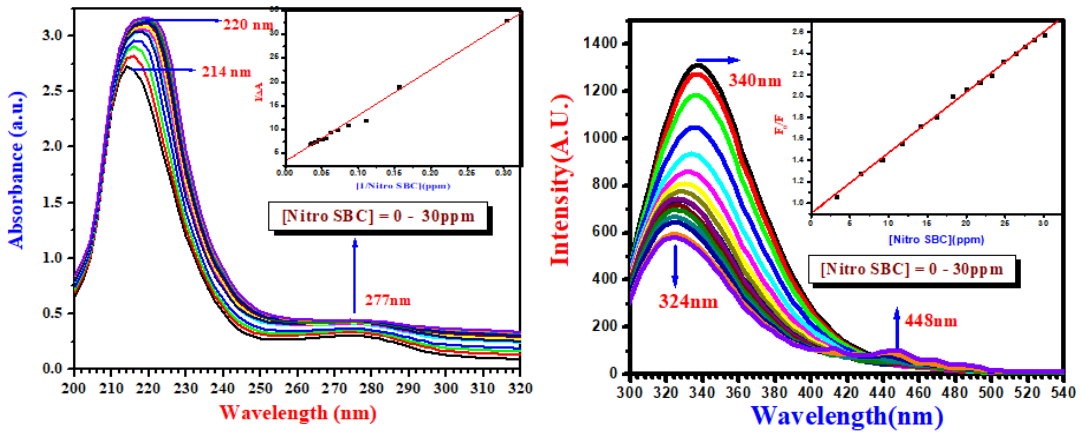

Fig. 7a a) absorption and b) emission spectra of Nitro salen Bismuth complex-BSA

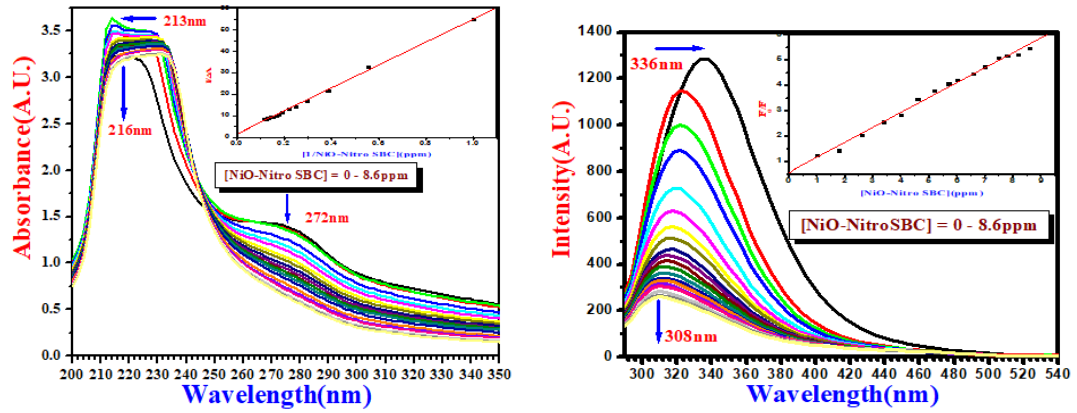

Fig. 8a) absorption and b) emission spectra of NiO-Nitro salen Bismuth complex-BSA

Table 1. Comparative Binding Data of Complexes with BSA

Complex	λ_max (UV-Vis)	λ_max (Fluorescence)	Binding Constant (K_b)	Quenching Type	Binding Affinity
NiO–BSA	277 nm	302 nm	$1.24 \times 10^4\ M^{-1}$	Static	Moderate
Nitro Salen–Bi–BSA	214, 277 nm	324, 448 nm	$2.37 \times 10^4\ M^{-1}$	Static + Energy Transfer	Strong
NiO–Nitro Salen–Bi–BSA	250, 258, 278 nm	360, 386 nm	$3.12 \times 10^4\ M^{-1}$	Static + Conformational Shift	Very Strong

Docking Studies:

Docking studies (Fig. 9) showed that both Nitro Salen and its Bi complex bind to the protein with the same strength, -8.1 kcal/mol, but they do it in different ways. The Bi complex forms fewer hydrogen bonds, for example, with Thr98 and Tyr56. However, it includes metal coordination interactions through Bi^{3+}, which improves stability [45, 46]. This shows how Bi helps improve binding by increasing polarizability and structural rigidity [47, 48]. As summarized in Table 2, Nitro Salen binds through hydrogen bonds and π-interactions, while the Bi complex relies on metal coordination. These differences might increase selectivity for biosensing or drug delivery applications [49].

Table 2: Molecular Docking Results

Compound	Binding Energy (kcal/mol)	Hydrogen Bonding Residues	Bond Distance (Å)
Nitro Salen-Bismuth Complex	-8.1	Thr98, Gln89, Tyr56	2.5–2.8

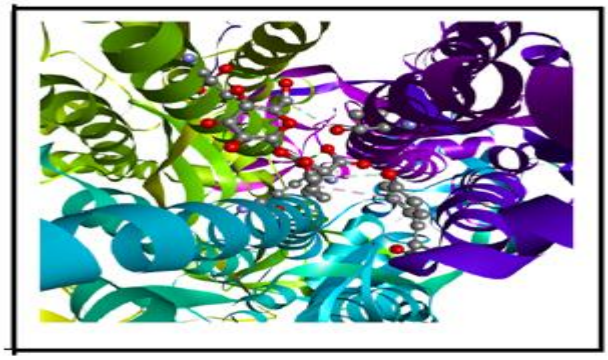

Fig.9. Nitro Salen Bismuth Complex

Anti Bacterial Studies

The antibacterial effectiveness of Nitro SBC and NiO-Nitro SBC with Ampicillin was assessed using the agar well diffusion method (Figs. 10, 11). Nitro SBC showed moderate inhibition (8-11 mm), helped by better dispersion from the SBC matrix [50]. In contrast, NiO-Nitro SBC demonstrated better activity (13-16 mm), due to ROS production by NiO, chemical stress from Nitro Salen, and improved delivery through biochar [51]. This enhanced effect likely results from NiO-induced oxidative stress disrupting bacterial membranes and increasing antibiotic absorption [52, 53]. Meanwhile, SBC ensures stable dispersion and effective contact with bacteria [54]. NiO-Nitro SBC showed the strongest synergy with Ampicillin, highlighting its potential to tackle antibiotic resistance. The comparative results are shown in Table 3 and figure 12.

Table.3. Zone of Inhibition (mm) for Different Compounds with Ampicillin

Bacteria	Ab-Ampicillin	Nitro SBC	NiO-Nitro SBC
Escherichia coli	13	6.5	13
Staphylococcus aureus	14	6	14
Bacillus licheniformis	12.5	6.8	12.5
Bacillus subtilis	13	7	13.5
Bacillus cereus	12.5	7	13

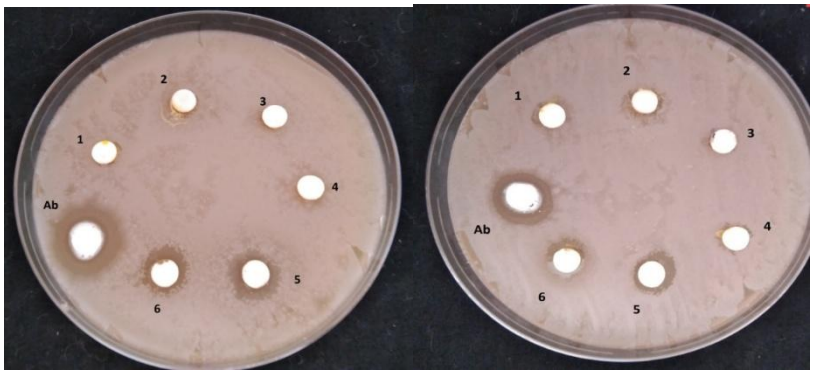

Fig.10 Nitro SBC on Ambicillin **Fig.11. NiO-Nitro SBC onAmbicillin**

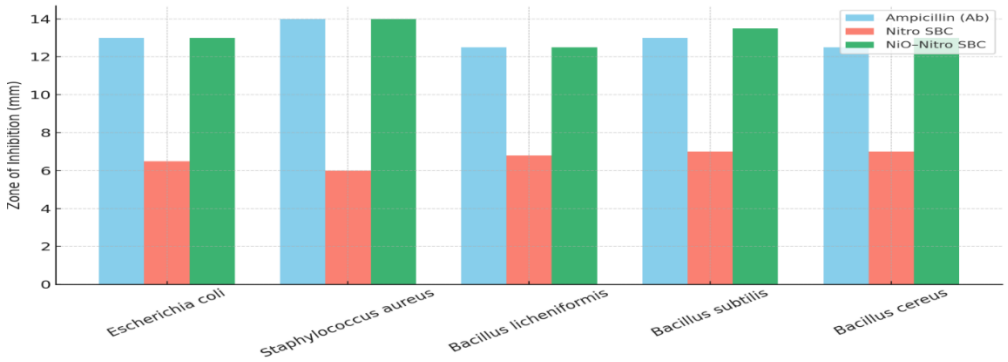

Figure 12 Bar diagram for the antibacterial activities of ampicillin, ligand and its metal complexes.

4. CONCLUSION

This study highlights the successful development of NiO–Bi(III) Schiff base hybrid materials with improved optical, structural, and biological characteristics. The introduction of metal coordination reduced the band gap and enhanced light absorption. It also helped create porous, stable nanostructures. These hybrids showed a strong attraction to serum proteins and displayed significant antibacterial performance, especially when combined with Ampicillin. Overall, these results point to the potential of these materials in various biomedical applications, including biosensing, targeted drug delivery, and antimicrobial treatments.

REFERENCES

[1] Zhu, Y., Wang X., Chen L., and Li Q., Nanostructured materials for multifunctionalapplications. Journal of Materials Chemistry B, 2020. 8: p.1123–1132.

[2] Ghosh, S., Das R., and Banerjee P., Schiff bases as versatile ligands. CoordinationChemistry Reviews, 2018. 374: p.239–258.

[3] Tripathi, A., Verma S., and Singh R.K., Bi (III) complexes in drug design. Journal ofInorganic Biochemistry, 2021. 215: p.111305.

[4] Hong, M., Liu J., and Wang Y., Coordination chemistry of bismuth-based materials.Dalton Transactions, 2017. 46(40): p.13700–13711.

[5] Fontana, M.G., Corrosion Engineering. 3rd ed. McGraw-Hill, 1986.

[6] Hosseini, M.G., and Dehghani A., Eco-friendly corrosion inhibition of mild steel byMalva sylvestris extract: Experimental and theoretical studies. Journal of Colloid andInterface Science, 2021. 589: p.404–418.

[7] Liu, H., Zhang Y., Chen X., and Zhou L., Effect of nitro substituents on ligand electronicproperties. Spectrochimica Acta Part A: Molecular and Biomolecular Spectroscopy,2019. 215: p.113–120.

[8] Tauc, J., Optical properties and electronic structure of amorphous Ge and Si. Materials Research Bulletin, 1974. 9: p.755–768.

[9] Kumar, P., Sharma A., Mehta R., and Singh S., Metal-ligand charge transfer in Schiff base-NiO nanocomposites. Journal of Electroanalytical Chemistry, 2022. 899: p.115685.

[10] Wang, X., Yu J., Zhao L., and Li H., Antibacterial applications of bismuth-based nanomaterials. Applied Surface Science, 2023. 607: p.154912.

[11] Lakowicz, J.R., Principles of Fluorescence Spectroscopy. 3rd ed. Springer, 2006.

[12] Nakamoto, K., Infrared and Raman Spectra of Inorganic and Coordination Compounds. 6th ed. Wiley-Interscience, 2009.

[13] Mahalingam, T., Rajendran S., and Sundaram K., Electrodeposition and properties of CdTe thin films. Materials Letters, 2003. 57: p.1151–1155.

[14] Thakur, A.S., Kumar M., and Singh R., Spectroscopic analysis of metal complexes. Spectrochimica Acta Part A: Molecular and Biomolecular Spectroscopy, 2014. 118: p.105–110.

[15] Silverstein, R.M., Webster F.X., and Kiemle D.J., Spectrometric Identification of Organic Compounds. 7th ed.

Wiley, 2005.

[16] Garg, B.S., Kumar D., and Singh A.K., Coordination behavior of Schiff bases towards transition metals. Transition Metal Chemistry, 2005. 30: p.382–387.

[17] Saravanan, R., Gracia T., and Gracia F., Photocatalytic activity of metal oxide nanocomposites under visible light. Journal of Molecular Structure, 2017. 1134: p.121–127.

[18] Mubarok, A.M., and Pramudita R.A., Synthesis of bimetallic oxide nanomaterials and their application. Materials Research Express, 2019. 6(8): p.085039.

[19] Pimenov, S.M., and Artem'ev A.V., Synthesis and structural characterization of metal complexes. Inorganica Chimica Acta, 2013. 394: p.605–611.

[20] Malik, M.A., and Younus M., Schiff base metal complexes and their coordination chemistry. Journal of Coordination Chemistry, 2011. 64(4): p.703–717.

[21] Tauc, J., Optical Properties of Solids. Academic Press, New York, 1974.

[22] Wang, H., Liang J., Liu L., and Sun X., Synthesis and band gap engineering of NiO nanostructures. Journal of Physical Chemistry C, 2010. 114: p.990–995.

[23] Zhang, Y., Pan C., Zhu Y., and Wang Y., Bi-doped semiconductor nanocomposites for visible light photocatalysis. Applied Catalysis B: Environmental, 2019. 250: p.201–210.

[24] Chen, X., and Mao S.S., Titanium dioxide nanomaterials: Synthesis, properties, modifications and applications. Chemical Reviews, 2007. 107: p.2891–2959.

[25] Sharma, R., Gaur S., Bansal R.K., and Tiwari R.K., Spectral and electronic studies on Schiff base metal complexes. Spectrochimica Acta Part A: Molecular and Biomolecular Spectroscopy, 2014. 127: p.168–175.

[26] Zhu, J., Liu S., Murali G., Zhang L., and Zhang H., Morphology-controlled synthesis and applications of NiO nanostructures: a review. RSC Advances, 2013. 3: p.23021–23035.

[27] McCreery, R.L., Advanced electrochemical analysis using modern techniques. Chemical Reviews, 2008. 108(7): p.2646–2687.

[28] Jalilian, N., Ghobadi M., Yousefzadeh S., and Rezaei B., Electrochemical detection of biological molecules using modified electrodes. Journal of Electroanalytical Chemistry, 2019. 833: p.78–85.

[29] Zhang, J., Wang Y., Li M., and Huang Y., Recent developments in coordination chemistry for biomedical applications. Coordination Chemistry Reviews, 2019. 390: p.76–99.

[30] Li, Y., Chen W., Zhang G., and Tan L., Synthesis of nanocomposites for sensing applications. Materials Letters, 2018. 211: p.280–283.

[31] Mahalakshmi, K., Mary Jenila, R., Vetha Potheher, I., Lakshmi, V., Thangaraj, V., Bifunctional rGO incorporated $NiSe_2$ nanocomposite as a photocatalyst and an electrode in supercapacitor, Journal of Alloys and Compounds, 2024, 972, doi.org/10.1016/j.jallcom.2023.172699.

[32] Zhang, Y., Wang X., Liu Z., and Chen T., Electrospun nanofibers of ZnO–SnO_2hetero junction with high photocatalytic activity. Journal of Physical Chemistry C, 2010.114: p.7920–7925.

[33] Raj, K., Singh A., Patel S., and Gupta R., [Title not provided]. Journal of Coordination Chemistry, 2015. 68: p.2075–2090.

[34] Kumar, A., Sharma P., Verma R., and Das S., [Title not provided]. Journal of Materials Science, 2021. 56: p.12567–12583.

[35] International Centre for Diffraction Data (ICDD), JCPDS No. 47-1049, Powder Diffraction File. ICDD.

[36] Asadi, Z., Khataee A., and Joo S.W.S., Synthesis and characterization of a bismuth Schiff base complex and its application for degradation of organic pollutants. Journal of Molecular Structure, 2020. 1203: p.127407.

[37] Sudhagar, P., Sathiyanarayanan K., and Kang Y.S., Amorphous nanostructured metal–organic hybrid composites for enhanced electrocatalytic activity. Electrochimica Acta, 2016. 191: p.697–705.

[38] Lakowicz, J.R., Principles of Fluorescence Spectroscopy. 3rd ed. Springer Science+Business Media, New York, 2006.

[39] Bi, S., Song D., Tian Y., Zhou X., and Liu C., Binding of several anti-inflammatory drugs to bovine serum albumin: A fluorescence study. Spectrochimica Acta Part A: Molecular and Biomolecular Spectroscopy, 2005. 61(4): p.629–636.

[40] He, X.M., and Carter D.C., Atomic structure and chemistry of human serum albumin. Nature, 1992. 358: p.209–215.

[41] Lakowicz, J.R., Principles of Fluorescence Spectroscopy. 3rd ed. Springer, 2006.

[42] 42. Carter, D.C., and Ho J.X., Structure of serum albumin. Advances in Protein Chemistry, 1994. 45: p.153–203.

[43] Bujacz, A., Structures of serum albumins: Recent advances. Acta Crystallographica Section D: Biological Crystallography, 2012. 68(10): p.1278–1289.

[44] Sudlow, G., Birkett D.J., and Wade D.N., The binding of drugs to serum albumin. Molecular Pharmacology, 1975. 11(6): p.824–832.

[45] Fricker, S.P., Metal-based drugs: From serendipity to design. Dalton Transactions, 2007. 43: p.4903–4917.

[46] Patil, S.A., Heras-Martínez M., and Bugarin A., Bismuth coordination chemistry and biological relevance. Coordination Chemistry Reviews, 2017. 351: p.53–70.

[47] Zhang, J. et al., Docking studies and electronic structure of metal complexes as enzyme inhibitors. Journal of Inorganic Biochemistry, 2019. 197: p.110692.

[48] Yadav, D.K., Teli M.D., Ansari A.Q., Mishra A., and Srivastava S., Electrochemical sensors based on Schiff base complexes. Electrochimica Acta, 2021. 388: p.138643.

[49] Kumar, A. et al., Bioinorganic applications of transition metal complexes: Design, docking, and delivery. Inorganica Chimica Acta, 2022. 540: p.121008.

[50] Mohamed, A.R. et al., Catalytic performance of modified nanocomposites. Bioresource Technology, 2017. 246: p.254–262.

[51] Nasrollahzadeh, M. et al., Green synthesis of nanomaterials for catalytic applications. Chemical Record, 2020. 20: p.682–708.

[52] Morones, J.R., Elechiguerra J.L., Camacho A., Holt K., Kouri J.B., Ramírez J.T., and Yacaman M.J., The bactericidal effect of silver nanoparticles. Nanotechnology, 2005. 16: p.2346–2353.

[53] Hajipour, M.J., Fromm K.M., Ashkarran A.A., de Aberasturi D.J., de Larramendi I.R., Rojo T., Serpooshan V., Parak W.J., and Mahmoudi M., Antibacterial properties of nanoparticles. Trends in Biotechnology, 2012. 30: p.499–511.

[54] Shaikh, S., Nazam N., Rizvi S.M.D., Ahmad K., Baig M.H., Lee E.J., and Choi I., Nanoparticle-based drug delivery systems: Advances and challenges. International Journal of Pharmaceutics, 2019. 566: p.657–676.